Effect of Ammonia Addition on the Synthesis of Carbon-doped ZnO/N Nanorod by Hydrothermal Method: Physicochemical and Electrochemical Properties

Parasdila, Hanaiyah
Department of Physics, Universitas Sebelas Maret

Adama Dina Panuntun
Department of Physics, Universitas Sebelas Maret

Purnama, Budi
Department of Physics, Universitas Sebelas Maret

Widiyandari, Hendri
Department of Physics, Universitas Sebelas Maret

https://doi.org/10.5109/7236879

出版情報：Evergreen. 11 (3), pp.2360-2366, 2024-09. 九州大学グリーンテクノロジー研究教育センター
バージョン：

Effect of Ammonia Addition on the Synthesis of Carbon-doped ZnO/N Nanorod by Hydrothermal Method: Physicochemical and Electrochemical Properties

Hanaiyah Parasdila[1], Adama Dina Panuntun[1], Budi Purnama[1], Hendri Widiyandari[1,2,*]

[1]Department of Physics, Universitas Sebelas Maret, Jl. Ir. Sutami 36A, Surakarta 57126, Indonesia

[2]Centre of Excellence for Electrical Energy Storage Technology, Universitas Sebelas Maret, Jl. Slamet Riyadi 435, Surakarta 57146, Indonesia

*Author to whom correspondence should be addressed:
E-mail: hendriwidiyandari@staff.uns.ac.id

(Received November 3, 2023; Revised June 24, 2024; Accepted September 7, 2024).

Abstract: In this research, carbon-doped ZnO/N (Zinc Oxide/Nitrogen) with nanorod structures were successfully synthesized using hydrothermal method by varying the ammonia molarites (1 M; 3 M; and 5 M). In the preparation, carbon-doped ZnO/N was produced by reacting $Zn(NO_3)_2 \bullet 6H_2O$; Urea; Citric Acid; and ammonia (NH_4OH) at 160 ^oC for 10 hours and calcinated at 600 ^oC for 2 hours as the carbonization process and marked as ZnO/N-C. The XRD analysis reveals that all of the samples' crystalline structures are almost hexagonal in shape, with crystalline sizes of 19.96 nm for ZnO/N-C (A-1M); 17.02 nm for ZnO/N-C (A-3M); and 25.11 nm for ZnO/N-C (A-5M). In the reverse hand, the images SEM results indicate that all of the sample morphology is nanorods, and the EDX test results confirm the chemical composition of all samples, which confirms that nitrogen and carbon were present. Electrochemical Impedance Spectroscopy (EIS) was used to assess the electrochemical characteristics to obtain the resistance coefficient transfer (R_{ct}) data. According to the EIS data analysis, the R_{ct} for the ZnO/N-C (A-1M), ZnO/N-C (A-3M), and ZnO/N-C (A-5M) samples are 339.8, 359.8, and 285.4 ohm, respectively. As a result, the sample that exhibits the lowest R_{ct} value will be a potential candidate for the most efficient of the electron transfer process.

Keywords: carbon-doped ZnO/N; ammonia (NH_4OH); hydrothermal method; electrochemical property

1. Introduction

In the fields of industry and technology, materials science is gaining prominent position. On top of that, as energy storage becomes prevalent in technology in increasing numbers globally, the demand for alternative energy sources, such as materials for battery components used in technology's energy storage as well as efficient energy transformation systems, is rising quickly. subsequently is therefore strongly advised to take on the challenge of discovering a new generation of energy storage sources. In addition to its intriguing properties as a material for research, ZnO has strong chemical and thermal stability, prolonged electron recombination, semiconductor, piezoelectric, and pyroelectric qualities, as well as reasonably cheap manufacturing costs[1-3], which have been reported It is expected that ZnO will become an excellent candidate material for energy storage applications.

According to research that have been published, ZnO has a number of benefits that make it a promising material for energy storage applications such as a material for Li-ion battery components. Because ZnO precursor is easy to prepare, affordable to produce, with good electrochemical qualities, non-toxic, and nanosized[4,5]. Recent years have brought about an enormous increase in the total amount of research being conducted to figure out ZnO's nanostructure due to the fact that is still much to learn concerning its wide range of potential applications across numerous industries. There are several methods to synthesize ZnO nanostructures, including sol-gel[6], electrodeposition[7], and hydrothermal/solvothermal[8].

The use of different synthesis methods and the variations used are reported to produce different morphological structures of ZnO materials[9]. From what other researchers have reported, ZnO has several morphologies, such as 1-D and 3-D forms[10]; nanoflakes[11]; and nanorods[12]. Furthermore, differences in ZnO nanostructure formation have demonstrated

significant differences in material physical characteristics, including surface area and electroactivity[13,14].

Based on other reports[15,16], ZnO exhibits low ionic weakness and extensive volume variations in its electrochemical characteristics, which lead to delayed reaction kinetics and poor electrochemical performance. In order to solve this problem, we examined the structure of the carbon-doped nanorod ZnO/N, which was synthesized by reacting citric acid ($C_6H_8O_7$) and urea ($CO(NH_2)_2$) in a hydrothermal method, and followed by the carbonization process, where carbon and nitrogen are supplied by citric acid and urea, respectively.

In this study, the addition of ammonia solution aims to modify the morphology in order to synthesize ZnO remaining directly. In this particular case, it is expected that the ZnO structure will change due to the fluctuations in ammonia addition. One common method for synthesizing ZnO in solution form is the addition of ammonia. Ammonia can additionally contribute in the formation of a stable Zn complex[17]. As a result, this study emphasizes the importance of ammonia concentration when producing ZnO. Several other researchers have previously reported on the treatment of ZnO for growth from aqueous solutions while taking into account the formation of Zn-ammonia complexes[18,19]. In addition, this study aims to prepare ZnO particles in carbon-doped ZnO/N to significantly improve its electrochemical properties.

2. Experimental

To prepare the carbon-doped ZnO/N nanorod was refer to Kim et al.[20] methods. Zinc nitrate hexahydrate ($Zn(NO_3)_2{\cdot}6H_2O$, Sigma Aldrich 98%), citric acid ($C_6H_8O_7$, PT. Brataco), urea ($CO(NH_2)_2$, Supelco), and ammonia solution 25% (NH_4OH, Supelco) was dispersed in distilled water 10 mL each. The molarity of the ammonia addition—1 M, 3 M, and 5 M—is where the variation in the solution will be observed. The formed solution was dropped wise into autoclave. The solution was then hydrothermally heated for 10 hours at 160ºC. The solution was then washed using distilled water and dried in the oven for 3 hours. The produced powder was loaded into furnace and calcinated at 600 ºC for 2h with a heating rate of 5ºC m^{-1}.

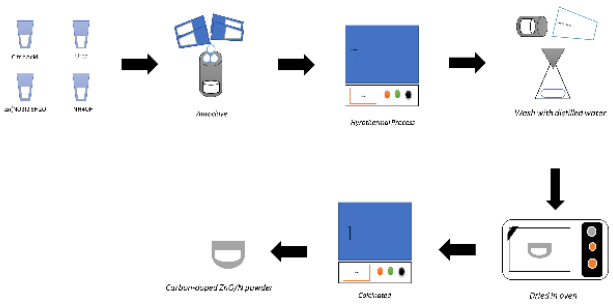

Fig. 1: Schematic diagram for the synthesis of carbon-doped ZnO/N nanorod

FE-SEM (Field Emission-Scanning Electron Microscopy) (FE-SEM, JEOL JIB-4610F), was used to examine the morphologies and microstructures of carbon-doped ZnO/N nanorods, Energy Dispersive X-Ray analysis (EDX, JEOL JIB-4610F) was used to obtain the elemental composition of the ZnO as well as the existence of impurities in the ZnO. The powder X-ray diffraction (XRD) patterns of the carbon-doped ZnO/N nanorod were obtained using an X-ray diffractometer (MTI, USA) with a diffraction angle (2θ) ranging from 170 to 70° at a rate of 0.05 s^{-1}. The electrochemical properties of carbon-doped ZnO/N nanorod was investigated using electrochemical impedance spectroscopy (EIS) (Pro Nuvant, China) to obtain the resistance coefficient transfer (R_{ct}) value with the frequency range of 0.01 Hz to10 kHz and the amplitude of 5 mV. Due to the produced carbon-doped ZnO/N's resistance being measured in this analysis utilizing the EIS instrument, a CR2025 type coin cell battery was constructed using the carbon-doped ZnO/N material (Fig. 2) by using $LiPF_6$ as the electrolytes.

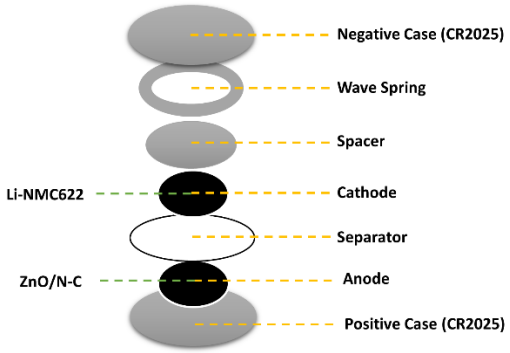

Fig. 2: Schematic diagram of the coin cell fabrication

3. Results and discussion

3.1 Crystal Structure

The XRD pattern of a carbon-doped ZnO/N nanorod is presented in **Fig. 3**. It is known from the XRD data results that all samples has the same peaks and the intensities of the sample is low, suggesting the presence of small particles[21]. All of the diffraction peaks can be precisely aligned to the (100), (002), (101), (102), (110), and (200) diffraction planes of the carbon-doped ZnO/N nanorod phase, whereas the 2Θ at 36º and others are associated to the hexagonal crystal structure of ZnO based on the International Centre for Diffraction Data (ICDD) number 89-1397 with the lattice parameters a = 3.253 Å and c = 5.213 Å and the hexagonality is 1.6. Hexagonality for all samples are 1.6, 1.59, and 1.59 based on the calculation of hexagonality from XRD data (Table 2). The obtained hexagonality indicates that it is in close proximity to the optimal value recorded in the ICDD database (number 89-1397).

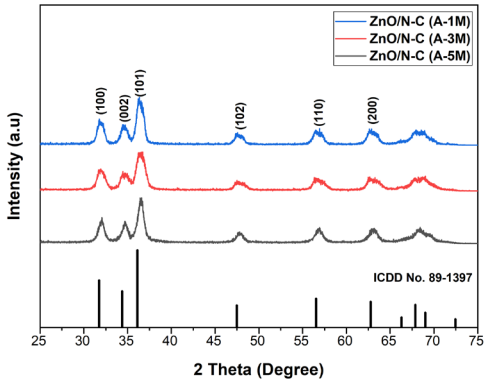

Fig. 3: XRD pattern of carbon-doped ZnO/N nanorod

Based on the calculation of the crystallite size using Scherrer equation (Table 1), it is found that the crystal size of carbon-doped ZnO/N nanorod tends to grow from 17.02 nm to 25.11 nm as the effect of the ammonia solution addition in the sample. Consequently, the ligand exchange reaction of the surrounding Zn-ammonia complexes into a complex hydroxide is what occurs when ammonia is added in order to induce the formation of ZnO crystals[22]. The Zn-hydroxide complex is the direct precursor for ZnO crystal growth and the concentration is much lower than the Zn-ammonia complex so that by given the molarity ratio of these two complexes, the numerous Zn-ammonia complexes nearby can be used in a ligand exchange reaction to make up for the Zn-hydroxide complex that is used for crystal formation[22].

The growth of ZnO crystals is influenced by molarity amount of the ammonia addition during synthesis. The following experiment should conduct a series of tests to investigate the impact of molarity amount of the ammonia addition on the procedure to get its best optimum[23]. All the calculated lattice parameters by using Bragg law are also close to the ideal values according to the ICDD database No. 89-1397 which indicates that ZnO has a hexagonal structure with the hexagonality close to the ideal hexagonal ZnO value at around 1.6 (**Table 2**).

Table 1. Crystallite size of carbon-doped ZnO/N nanorod

Sample	NH_4OH molarity (M)	2Θ (°)	D (nm)
ZnO/N-C (A-1M)	1	36.43	19.96
ZnO/N-C (A-3M)	3	36.50	17.02
ZnO/N-C (A-5M)	5	36.51	25.11

Table 2. Lattice parameter of carbon-doped ZnO/N nanorod

Sample	a (Å)	c (Å)	Hexagonality (c/a)
ZnO/N-C (A-1M)	3.48	5.58	1.6
ZnO/N-C (A-3M)	3.47	5.55	1.59
ZnO/N-C (A-5M)	3.47	5.55	1.59

3.2 Morphology

Figure 4 (a-c) shows the SEM image of all samples presented in **Fig. 4**(a-c), it can be seen that all structures are nanorods with non-uniform size distribution. Based on the previous report Jang[24], the surface energy of the [0001] plane is greater than that of the nonpolar [1010] and [1120] fields. This is due to the fact that crystal growth is more rapid in the [0001] direction. The area of [0001] then decreases as the ZnO crystal grows, resulting in the formation of hexagonal ZnO nanorods[24].

In the non-uniform particle size shown in **Fig. 5** (a-c), the dominant particle average diameter at the range of 118-165 nm. It is found that ZnO nanorod structure grew, as the ammonia molarity increased, causing the ZnO rod structure to form shorter rods. The average value of the particle diameter obtained from the SEM images using ImageJ software decreases with increasing ammonia molarity, namely 165 nm (ZnO/N-C (A-1M)); 146 nm (ZnO/N-C (A-3M)); and 118 nm (ZnO/N-C (A-1M)).

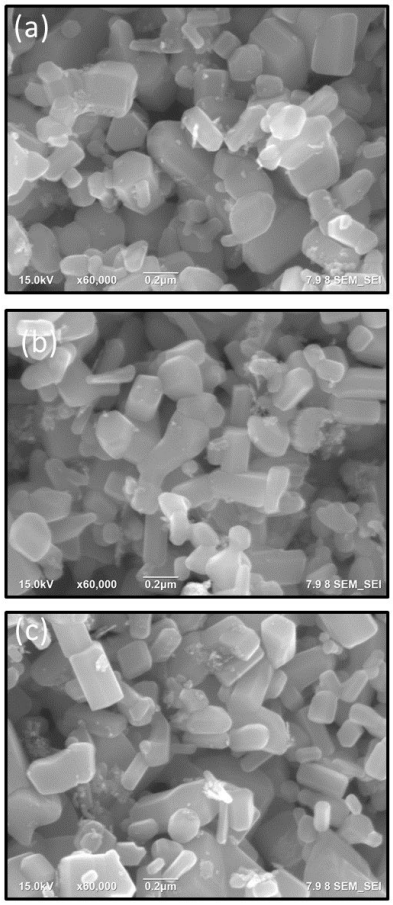

Fig. 4: FE-SEM image (a) ZnO/N-C (A-1M); (b) ZnO/N-C (A-3M); and (c) ZnO/N-C (A-5M)

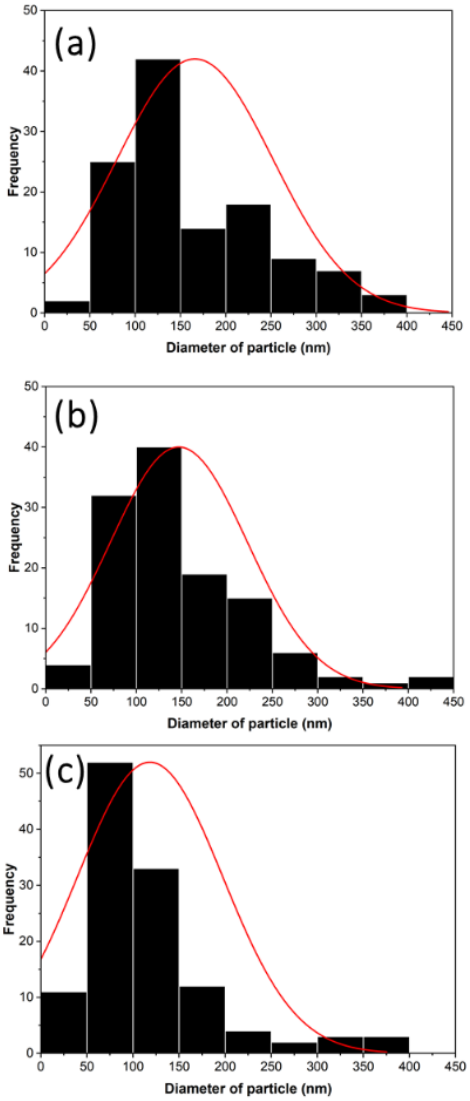

Fig. 5: Particle size of (a) ZnO/N-C (A-1M); (b) ZnO/N-C (A-3M); and (c) ZnO/N-C (A-5M)

Table 3. Chemical elements contained in carbon-doped ZnO/N nanorod

Sample	NH_4OH molarity (M)	Element (%)			
		Zn	O	C	N
ZnO/N-C (A-1M)	1	71.61	20.97	7.15	0.27
ZnO/N-C (A-3M)	3	77.99	3.39	5.16	0.05
ZnO/N-C (A-5M)	5	97.63	1.01	1.11	0.25

Table 3 shows the EDX analysis of the carbon-doped ZnO/N. It is evident that all samples proving the presence of Zn, O, C, and N. ZnO/N-C (A-5M), the sample with the highest ammonia molarity, had the highest percentage of Zn, whereas ZnO/N-C (A-1M) had the lowest percentage. As the molarity of ammonia increased, the percentage of Zn in each sample increased as well. Conversely, the percentage of element O obtained was highest in the ZnO/N-C sample (A-1M) and lowest in the ZnO/N-C sample (A-5M). Carbon-doped ZnO/N nanorods were successfully synthesized, according to the EDX results.

3.3 FT-IR Spectra

The FTIR spectra before and after calcination were tested in the range of 400 and 4000 cm^{-1} (**Fig. 6**(a-b)). The FTIR spectrum before calcination (Fig. 6(a)), show that various functional group peaks and metal oxide bonds present in the compound were detected. A significant and the characteristic strain mode of the Zn-O bond is showed vibrational band ranging from 400 cm^{-1} to 500 cm^{-1} [25,26]. The broad and small peaks at around 3609, 3428, and 3263 cm^{-1} are due to the presence of O-H groups and the CO_2 strain mode. The 868 cm^{-1} band is showed due to the formation of Zn which will be tetrahedral coordinated. Then, around 1575 and 1408 cm^{-1}, it is suspected that they are related to the symmetrical and asymmetric stretching vibrations of the carboxylate groups from the originating reaction intermediate or small residues of zinc nitrate used in the production of ZnO nanoparticles[27,28]. There were several small absorption bands at 697, 762, and 1024 cm^{-1} that are likely related to CO_2 (C–O) and H_2O (O–H) absorbed from the atmosphere (air), and these absorption bands can be neglected[29].

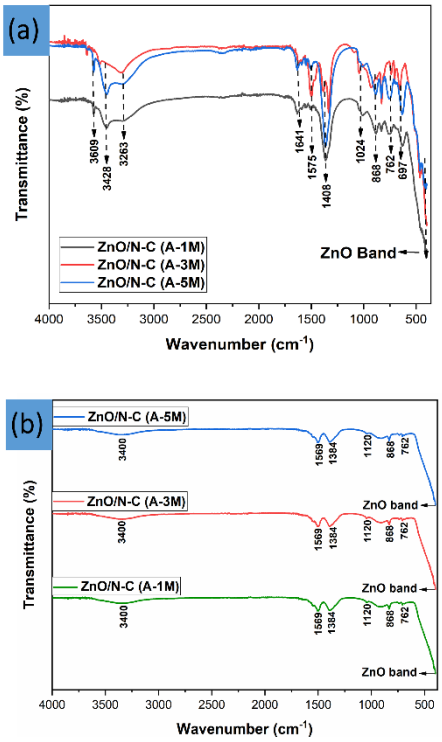

Fig. 6: (a) FTIR spectra before calcinated; (b) FTIR spectra after calcinated

When carbon-doped ZnO/N nanorod samples were calcined to 600°C, several peaks were lost (Fig. 6(b)); some of the missing bands were caused by evaporation of

water to the surface and decomposition of the carbon matrix.The carbon-doped ZnO/N nanorods, on the other hand, had a high intensity in the 3400 cm^{-1} band. where the presence of N-H stretching vibrations is indicated some additional bands at 1100-1200 cm^{-1}, which peak at 1569 cm^{-1} for C-C and C-N stretch vibrations, according to the C-C, C-O, and C-N strain vibrations[20].

3.5 Electrochemical Properties

To examine the electrochemical properties of carbon-doped ZnO/N, the sample were assembled into the coin cells (CR2025) in a glove box. The electrochemical properties test was only carried out by analyzing the Nyquist plot of all samples to determine R_{ct} value of the samples.

Based on **Figure 7**, the Nyquist plot was fitted with data to find the equivalent series for carbon-doped ZnO/N nanorod. It is noted that the there is a discrepancy at low frequencies between the fitting results (green line) and the experimental data is due to the data has been normalized automatically by the Zsimp 3.2 software to find the circuit that has closest values to the experimental data.

According to the results, it is found that the respective R_{ct} values obtained are 339.8 ohms (ZnO/N-C (A-1M)), 359.8 ohms (ZnO/N-C (A-3M)), and 285.4 ohms (ZnO/N-C (A-5M)). Based on the findings by Ahmad et al.[30] with ZnO samples with the same morphology, namely, nanorod, the best R_{ct} is (410 ± 23.6 ohms). Where in this study, it was found that the lowest R_{ct} value was 285.4 ohms, lower R_{ct} value than reported in. Low-resistance materials have optimal performance in lithium-ion transfer rates during intercalation process [31]. Based on XRD result, carbon-doped ZnO/N sample with the addition of 5 M of ammonia (ZnO/N-C (A-5M)) is also the sample with most crystalline of the other two samples. With the increasing in the crystal size, it means space for the intercalation of lithium ions to facilitate the rate of ion transfer is also accelerating. The ZnO nanostructure has resulted in an increasing crystallinity of carbon-doped ZnO/N, which also improves ZnO's electrochemical properties[32,33].

When it seen from the morphology of the SEM result, carbon-doped ZnO/N sample with the addition of 5 M molarity of ammonia (ZnO/N-C (A-5M)) has the smaller particles which will later expand the space for intercalation during electrochemical impedance testing[34,35]. It can be concluded that the carbon-doped ZnO/N sample with the addition of 5 M of ammonia (ZnO/N-C (A-5M)) is the best candidate to be a material that will be applied as an energy storage material such as lithium-ion battery electrodes.

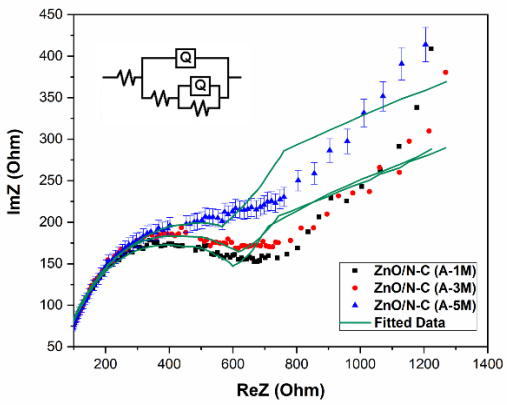

Fig. 7: Nyquist plot of carbon-doped ZnO/N nanorod

4. Conclusions

The carbon-doped ZnO/N nanorod was successfully prepared by varying the molarity of ammonia through a hydrothermal process. All of the XRD results revealed that all carbon-doped ZnO/N samples were hexagonal and had crystal peaks that matched the ICDD database. All samples of carbon-doped ZnO/N sample possesses a nanorod structure, with an average diameter ranging from 118 nm to 165 nm. All carbon-doped ZnO/N nanorod samples have been successfully synthesized with nitrogen and carbon elements, as confirmed by the EDX results. Sample ZnO/N-C (A-5M) has the best R_{ct} value of 285.4 ohms, it can be taken into consideration as a potential material for energy storage.

Acknowledgements

The authors thank to Centre of Excellence for Electrical Energy Storage Technology, Universitas Sebelas Maret Surakarta for all the facilities for characterization.

References

1) S. Wei, S. Wang, Y. Zhang, and M. Zhou, "Different morphologies of ZnO and their ethanol sensing property," Sensors and Actuators B: Chemical, vol. 192, pp. 480-487, 2014.
2) D. Widhiyanuriyawan, Z. Arifin, A. Muwaffaq, S. Suyitno, S. Hadi, S. D. Prasetyo, & B. Sutanto. "The Effect of Electrospinning Precursor Flow Rate with Rotating Collector on ZnO Nanofiber Size Results on Double-Layered DSSC Photoanode Fabrication." *Evergreen*, 10(1), pp. 504-509, 2023. Doi: doi.org/10.5109/6782154
3) A. S. Rini, Y. Rati, R. Fadillah, R. Farma, L. Umar & Y. Soerbakti. "Improved Photocatalytic Activity of ZnO Film Prepared via Green Synthesis Method Using Red Watermelon Rind Extract." *Evergreen*, 9(4), pp. 1046-1055, 2022. Doi: doi.org/10.5109/6625718
4) W. Mai, Z. Liang, L. Zhang, X. Yu, P. Liu, H. Zhu, X. Chai, & Tan, S. Strain sensing mechanism of the

fabricated ZnO nanowire-polymer composite strain sensors. Chemical Physics Letters, 538, 99-101. (2012). doi: 10.1016/j.cplett.2012.04.041

5) T. L. H. Doan, J. Y. Kim, J. H. Lee, L. H. T. Nguyen, H. T. T. Nguyen, A. T. T. Pham, T. B. L. Nguyen, M. Ali, T. B. Phan, & S. S. Kim. Facile synthesis of metal-organic framework-derived ZnO/CuO nanocomposites for highly sensitive and selective H2S gas sensing. Sensors and Actuators B: Chemical, 349, 130741. (2021). doi: 10.1016/j.snb.2021.130741
6) S. Jurablu, M. Farahmandjou, & T. P. Firoozabadi, Sol-gel synthesis of zinc oxide (ZnO) nanoparticles: study of structural and optical properties. Journal of Sciences, Islamic Republic of Iran, 26(3), 281-285. (2015).
7) M. Lüsi, H. Erikson, M. Merisalu, M. Rähn, V. Sammelselg, & K. Tammeveski. Electrochemical reduction of oxygen in alkaline solution on Pd/C catalysts prepared by electrodeposition on various carbon nanomaterials. Journal of Electroanalytical Chemistry, 834, 223-232. (2019). doi: 10.1016/j.jelechem.2018.12.061
8) H. Wang, T. Liang, X. Yu, W. Zhao, R. Xu, D. Wang, & Y. Liu. Hydrothermal synthesis of well-crystallized CuO hierarchical structures and their direct application in high performance lithium-ion battery electrodes without further calcination. RSC advances, 6(99), 96882- 96888. (2016). doi: 10.1039/C6RA20701D
9) P. Obreja, D. Cristea, A. Dinescu, & C. Romaniţan. Influence of surface substrates on the properties of ZnO nanowires synthesized by hydrothermal method. Applied Surface Science, 463, 1117-1123. (2019). doi: 10.1016/j.apsusc.2018.08.191
10) S. Wahyuningsih, A. H. Ramelan, E. Pramono, H. P. Nuryana, M. M. A. Mujahidin, H. Munawaroh, R. Hidayat, & G. Fadillah. Transformation growth of nanoflower-like GO-ZnO as an active site platform for H2S sensors. Chemical Physics Letters, 790, 139351. (2022). doi: 10.1016/j.cplett.2022.139351
11) Y. Yan, B. Wang, C. Yan, & D. J. Kang. Decorating ZnO nanoflakes on carbon cloth: Free-standing, highly stable lithium-ion battery anodes. Ceramics International, 45(13), 15906-15912. (2019).
12) P. Cao, Z. Yang, S. T. Navale, S. Han, X. Liu, W. Liu, F. J. Stadler, & D. Zhu. Ethanol sensing behavior of Pd-nanoparticles decorated ZnO-nanorod based chemiresistive gas sensors. Sensors and Actuators B: Chemical, 298, 126850. (2019). doi: 10.1016/j.snb.2019.126850
13) C. K. Zagal-Padilla, C. Diaz-Gómez, & S. A. Gamboa. Electrochemical characterization of a plasmonic effect ethanol sensor based on two-dimensional ZnO synthesized by green chemistry. Materials Science in Semiconductor Processing, 137, 106240. (2022). Doi: 10.1016/j.mssp.2021.106240
14) M. Ebrahimi, A. Bayat, S. R. Ardekani, E. S. Iranizad, & A. Z. Moshfegh. Sustainable superhydrophobic branched hierarchical ZnO nanowires: Stability and wettability phase diagram. Applied Surface Science, 561, 150068. (2021). Doi: 10.1016/j.apsusc.2021.150068
15) C. Q. Zhang, J. P. Tu, Y. F. Yuan, X. H. Huang, X. T. Chen, & F. Mao. Electrochemical performances of Ni-coated ZnO as an anode material for lithium-ion batteries. Journal of the Electrochemical Society, 154(2), A65. (2006). Doi: 10.1149/1.2400609
16) H. Kim, W. Jae, J. Song, & J. Kim. Skein-shaped ZnO/N-doped carbon microstructures as a high performance anode material for lithium-ion batteries. Journal of Alloys and Compounds, 772, 507-515. (2019). Doi: 10.1016/j.jallcom.2018.09.198
17) J. J. Richardson, & F. F. Lange. Controlling low temperature aqueous synthesis of ZnO. 1. Thermodynamic analysis. Crystal Growth and Design, 9(6), 2570-2575. (2009). Doi: 10.1021/cg900082u
18) A. M. Chaparro, Thermodynamic analysis of the deposition of zinc oxide and chalcogenides from aqueous solutions. Chem. Mater. 17 (16), 4118–4124. (2005). Doi: 10.1021/cm0502323
19) C. Hubert, N. Naghavi, B. Canava, A. Etcheberry, D. Lincot. Thermodynamic and experimental study of chemical bath deposition of Zn(S, O, OH) buffer layers in basic aqueous ammonia solutions. Cell results with electrodeposited CuIn(S, Se)(2) absorbers. Thin Solid Films. 515 (15), 6032–6035. (2007). Doi: 10.1016/j.tsf.2006.12.139
20) H. Kim, W. Jae, J. Song, & J. Kim. Skein-shaped ZnO/N-doped carbon microstructures as a high performance anode material for lithium-ion batteries. Journal of Alloys and Compounds, 772, 507-515. (2019). Doi: 10.1016/j.jallcom.2018.09.198
21) B. Xie, A. Kitajou, S. Okada, W. Kobayashi, M. Okada, & T. Takahara. Cathode Properties of Na_3MPO_4CO_3 (M= Co/Ni) Prepared by a Hydrothermal Method for Na-ion Batteries. *Evergreen*, 6(4), 262-266. (2019). Doi: 10.5109/2547345
22) X. Gao, X. Li, & W. Yu. Synthesis and characterization of flowerlike ZnO nanostructures via an ethylenediamine-meditated solution route. Journal of Solid State Chemistry, 178(4), 1139-1144. (2005). Doi: 10.1016/j.jssc.2004.10.020
23) R. T. Ghahrizjani, & M. H. Yousefi. Effects of three seeding methods on optimization of temperature, concentration and reaction time on optical properties during growth ZnO nanorods. Superlattices and Microstructures, 112, 10-19, (2017). Doi: https://doi.org/10.1016/j.spmi.2017.08.041
24) E. S. Jang. Recent progress in synthesis of plate-like ZnO and its applications: a review. Journal of the Korean Ceramic Society, 54(3), 167-183. (2017). Doi: 10.4191/kcers.2017.54.3.04
25) Hower, P. L., & Gupta, T. K. A barrier model for ZnO

varistors. Journal of Applied Physics, 50(7), 4847-4855. (1979). Doi: 10.1063/1.326549
26) R. Wahab, S. G. Ansari, Y. S. Kim, H. K. Seo, G. S. Kim, G. Khang, & H. S. Shin. Low temperature solution synthesis and characterization of ZnO nano-flowers. Materials Research Bulletin, 42(9), 1640-1648. (2007). Doi: 10.1016/j.materresbull.2006.11.035
27) S. Udayakumar, V. Renuka, K. Kavitha, Structural, optical and thermal studies of cobalt doped hexagonal ZnO by simple chemical precipitation method, J. Chem. Pharm. Res. 4 (2) 1271–1280. (2012).
28) K. Ravichandrika, P. Kiranmayi, R.V.S.S.N. Ravikumar, Synthesis, characterization and antibacterial activity of ZnO nanoparticles, Int. J. Pharm. Pharm. Sci. 4 (4), 336–338. (2012).
29) D. Nipane, S. R. Thakare, & N. T. Khati. Synthesis of novel ZnO having cauliflower morphology for photocatalytic degradation study. Journal of Catalysts, (2013). Doi: 10.1155/2013/940345
30) R. Ahmad, M. S. Ahn, & Y. B. Hahn. A highly sensitive nonenzymatic sensor based on Fe2O3 nanoparticle coated ZnO nanorods for electrochemical detection of nitrite. Advanced Materials Interfaces, 4(22), 1700691. (2017). Doi: 10.1002/admi.201700691
31) A. H. Wibowo, H. Al Arraf, A. Masykur, F. Rahmawati, M. Firdaus, F. Pasila, P. Ulya, & N. Nasori. Composite of polyaniline/reduced graphene oxide with the single-, bi-and tri-metal oxides modification and the effect on the capacitance properties. *Evergreen*. *10*(1). 85-93, (2023). Doi: https://doi.org/10.5109/6781053
32) R. N. Anisa, S. Y. Cornelius, R. Mintarsih, S. N. Shofirul, J. Arif, H. Widiyandari, & A. Purwanto. Structural and Electrochemical Analysis of Iron Doping in LiNi_0. 6-x Mn_0. 2 Co_0. 2 Fe_x O_2 battery. *Evergreen*, *8*(1), 82-88. (2021). Doi: 10.5109/4372263
33) N. Siregar. (2023). Synthesis of ZnO Thin Film by Electroplating: Effect of Zinc Concentration on the Structural and Optical Properties. *Evergreen*. 10(2), 715-721, (2023). Doi: https://doi.org/10.5109/6792820
34) E. R. Dyartanti, I. N. Widiasa, A. Purwanto, & H. Susanto. Nanocomposite Polymer Electrolytes in PVDF/ZnO Membranes Modified with PVP for LiFePO_4 Batteries. *Evergreen. 5*(2), 19-25. (2018). Doi: 10.5109/1936213
35) Y. Liu, S. P. Jiang, & Z. Shao. Intercalation pseudocapacitance in electrochemical energy storage: recent advances in fundamental understanding and materials development. *Materials Today Advances*. 7, 100072, (2020). Doi: https://doi.org/10.1016/j.mtadv.2020.100072